Proceedings of the 9th Diesel Engine Emissions Reduction Conference
August 24-28, 2003, Newport, Rhode Island

NEW CORDIERITE DIESEL PARTICULATE FILTERS FOR CATALYZED AND NON-CATALYZED APPLICATIONS

Gregory A. Merkel, Willard A. Cutler and Tinghong Tao
Corning Incorporated

Andrew Chiffey, Paul Phillips, Martyn V. Twigg, and Andrew Walker
Johnson Matthey

ABSTRACT

Cordierite diesel particulate filters provide an economical approach to diesel emissions control. However, further reduction in the pressure drop of catalyzed and non-catalyzed cordierite filters is desirable. In order to derive a fundamental understanding of the relationship between clean and soot-loaded pressure drop and the pore microstructure of the ceramic, and to optimize the microstructure for filter performance, cordierite filters have been fabricated spanning an extended range in porosity, pore size distribution, and pore connectivity. Analysis of the results has been applied to the development of several new cordierite diesel particulate filters that possess a unique combination of high filtration efficiency, high strength, and very low clean and soot-loaded pressure drop. Furthermore, catalyst systems have been developed that result in a minimal pressure drop increase of the catalyzed filter. Optimization of porosity and cell geometry has enabled fabrication of filters with either high or low thermal mass appropriate to the regeneration strategy employed for a given engine management system.

Keywords: Cordierite, diesel particulate filter, porosity, pressure drop, catalyst

INTRODUCTION

Ceramic wall-flow diesel particulate filters (DPFs) are presently being implemented for the collection and combustion of carbonaceous soot from the exhaust of both light-duty and heavy-duty diesel engine vehicles. Optimum filter performance during the soot accumulation and soot combustion stages requires tailoring of the pore microstructure of the ceramic walls and the external dimensions and cell geometry of the filter.

To minimize reduction in vehicle power, it is important for the DPF to have a low pressure drop in the clean and soot-loaded states. Furthermore, depending upon the type of engine and the strategy employed to initiate regeneration of the filter, DPFs may be catalyzed to promote oxidation of CO and hydrocarbons, as well as to lower the temperature required for regeneration by soot combustion. Catalyzing the filter can further contribute to an increase in pressure drop across the filter.

In addition to the pressure drop of a filter, the volumetric heat capacity, or "thermal mass," of the filter, is also of importance. Requirements for thermal mass depend upon the engine operating conditions and regeneration strategy employed for a specific diesel vehicle. In the case of active regeneration, low thermal mass filters have the advantage of requiring a lower energy input to raise the temperature of the filter to the ignition temperature of the deposited soot. Likewise, under passive regeneration conditions, a filter with a low volumetric heat capacity will achieve the soot combustion temperature more frequently during the duty cycle of the engine, reducing the likelihood of high soot loading between successive regenerations. However, in applications in which there is the possibility of an occasional uncontrolled regeneration at high soot loading and low exhaust flow rate that would create a large exotherm over a short time interval, high thermal mass offers protection against excessive heating of the filter and catalyst system, preventing damage to the filter and deactivation of the catalyst.

The present study was undertaken in an effort to provide cordierite diesel particulate filters that offer low pressure drop in both low and high thermal mass configurations.

PRESSURE DROP - GENERAL OBSERVATIONS

The mechanisms by which pressure drop increases with progressive soot loading have been discussed previously by, for example, Murtagh et al. [1] and Masoudi et al. [2]. A generalized pressure drop versus soot loading curve for a given gas flow rate is depicted in Figure 1. The pressure drop at moderate to high soot loadings can be considered to be the sum of four components, or stages, along the pressure drop versus soot loading curve. The initial pressure drop of the clean filter (Stage 1), is controlled, in part, by the intrinsic permeability of the ceramic that comprises the filter. During the early stages of

soot loading in a filter in which large pores are present and which intersect the surface of the inlet channel walls, soot may accumulate on the walls of these pores. This causes a constriction in the pore diameters, but produces only a gradual decrease in wall permeability and a small increase in pressure drop (Stage 2). However, once the soot bridges the width of the surface pores so that the surface and near-surface pores become plugged with soot, the permeability of the wall is substantially reduced, resulting in a steep rise in pressure drop (Stage 3). In filters lacking a substantial population of large pores, the pressure drop curve is typically observed to go directly from Stage 1 to Stage 3. Eventually, the soot accumulates as a discrete layer, or "cake", on the surface of the inlet channel walls, and the pressure drop increase per unit mass of soot decreases to a steady state rate (Stage 4).

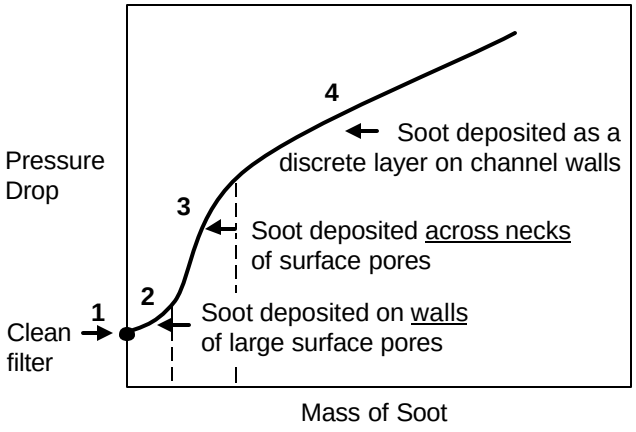

Figure 1. Schematic illustration of the increase in pressure drop with soot loading of a wall-flow diesel particulate filter. Numbers denote stages referred to in discussion.

EXPERIMENTAL STUDY OF PRESSURE DROP VERSUS PORE MICROSTRUCTURE

In an effort to understand how clean and soot-loaded pressure drop are influenced by the pore microstructure of the ceramic filter, and to develop a filter having an optimized pore microstructure for low pressure drop, a study was undertaken in which a series of cordierite ceramic filters was prepared with over one hundred different porosities and pore size distributions. The pore microstructures were characterized by mercury porosimetry. For each sample, the percent porosity and the pore diameters at 10%, 50%, and 90% of the cumulative pore size distribution, based upon pore volume, were recorded. These pore diameters are designated as d_{10}, d_{50}, and d_{90}, with d_{50} being the median pore diameter, and $d_{10} < d_{50} < d_{90}$.

The percent porosities of these materials are plotted against the median pore diameters in Figure 2. Porosities ranged from 36 to 66%, and median pore diameters from 4 to 38 microns.

The quantity $(d_{50}-d_{10})/d_{50}$ is plotted against median pore diameter in Figure 3. This parameter is a measure of the width of the fine end of the pore size distribution, $d_{50}-d_{10}$, normalized by dividing by d_{50} so that two ceramics having pore size

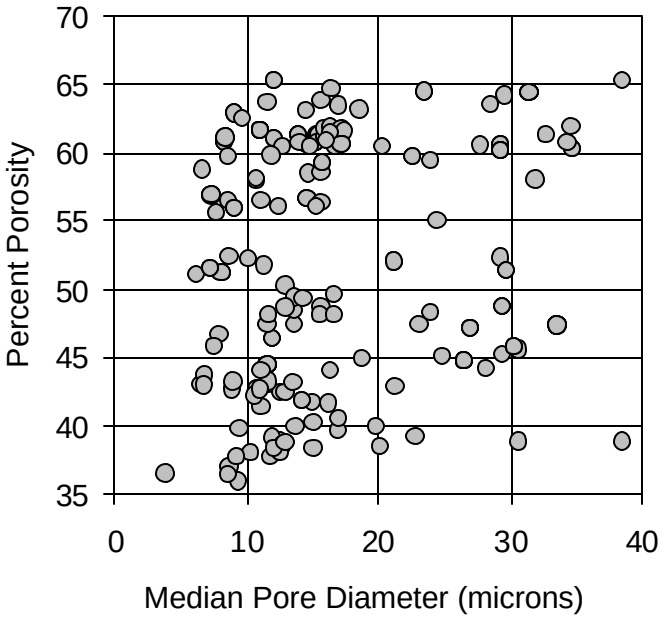

Figure 2. Plot of percent porosity versus median pore diameter for experimental cordierite filters fabricated to quantify the relationship between pressure drop and pore microstructure of bare filters.

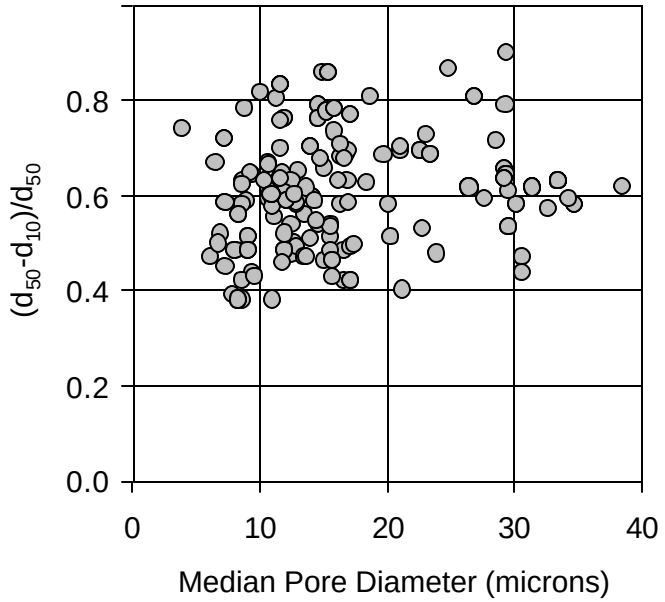

Figure 3. Plot of the $(d_{50}-d_{10})/d_{50}$ pore size distribution parameter versus median pore diameter for experimental cordierite filters fabricated to quantify the relationship between pressure drop and pore microstructure of bare filters.

distributions that differ only in scale would have the same value for $(d_{50}-d_{10})/d_{50}$. The maximum value that is theoretically achievable for $(d_{50}-d_{10})/d_{50}$ is 1.0, corresponding to a very broad pore size distribution with many extremely fine pores relative to the median pore size. The minimum theoretical value is 0.0, which would exist for a body comprised of uniform cylindrical

capillary pores. It was this quantity, rather than $(d_{90}-d_{10})/d_{50}$ or $(d_{90}-d_{50})/d_{50}$, that was observed to correlate with the soot-loaded pressure drop values.

These cordierite ceramics were fabricated as 2-inch diameter, 6-inch long filters with cell densities of approximately 200 cells inch^{-2} and wall thicknesses ranging from 0.008 to 0.026 inches. The clean and soot-loaded pressure drops of the filters were measured at room temperature and air flow rates of 1.9 to 26.25 standard cubic feet per minute (scfm), equivalent to space velocities of approximately 10,000 to 150,000 hr^{-1}. Artificial soot (Degussa Printex-U) was deposited at 15 scfm at levels ranging from approximately 0.5 to 5.0 grams/liter.

The relationships of clean and soot-loaded pressure drops to the %porosity, median pore diameter, and width of the pore size distribution were derived by multiple linear regression analysis of the data.

For a given filter cell geometry, clean pressure drop was found to be inversely proportional to the product (%porosity)$(d_{50})^2$. This observation is consistent with models for fluid flow through cylindrical capillary pores [3]. Because median pore size varied by a factor of almost ten in the present study, whereas %porosity varied by slightly less than a factor of two, and because the clean pressure drop is inversely related to the square of d_{50}, the pore size has a much greater effect on the clean pressure drop than does the %porosity, especially at median pore sizes less than about 7 microns below which the clean pressure drop increases steeply with decreasing pore size.

The soot-loaded pressure drop and, in particular, the rate of pressure drop increase during the initial stages of soot loading during which the soot is depositing within the surface and near-surface pores, was found to be minimized for high %porosity and small values of $(d_{50}-d_{10})/d_{50}$. It is believed that both high porosity and narrow pore size distribution contribute to a higher degree of pore connectivity. This should result in lower local gas velocities through the necks between the pore bodies within the wall, and less dense packing of the soot in the surface and near-surface pores. The less densely packed soot within the pores would, in turn, have a higher permeability, resulting in a more gradual increase in pressure drop with initial soot loading.

The influence of $(d_{50}-d_{10})/d_{50}$ and %porosity on clean and soot-loaded pressure drop is shown in Figures 4 and 5. These curves were computed from the regression equations for clean and soot-loaded pressure drop as a function of the pore parameters. Calculations were made assuming a 2-inch diameter, 6-inch long filter having 200 cells/in^2 and 0.012-inch thick walls, at a room-temperature air flow rate of 26.25 scfm. A decrease in $(d_{50}-d_{10})/d_{50}$ or an increase in %porosity substantially reduces the initial rate of pressure drop increase with soot loading, resulting in a desirably flatter pressure drop versus soot loading curve, while having a negligible effect on the clean pressure drop.

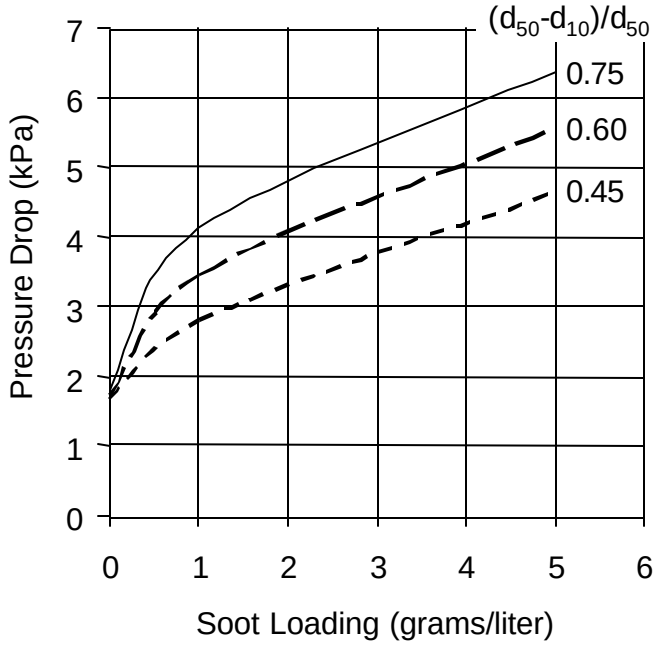

Figure 4. Pressure drops predicted from regression equations for clean and soot-loaded non-catalyzed cordierite filters as a function of the value of $(d_{50}-d_{10})/d_{50}$ assuming 50% porosity and a median pore size of 12 microns.

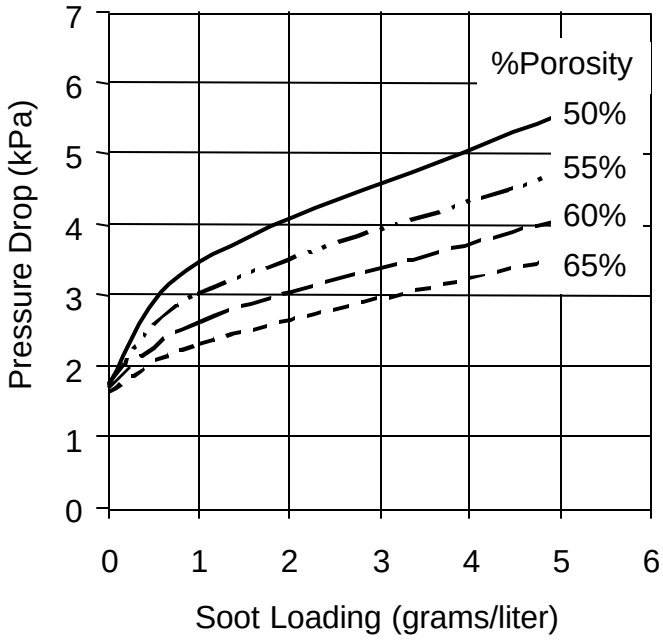

Figure 5. Pressure drops predicted from regression equations for clean and soot-loaded non-catalyzed cordierite filters as a function of the value of %porosity assuming a value of 0.60 for $(d_{50}-d_{10})/d_{50}$ and a median pore size of 12 microns.

PRESSURE DROP OF CATALYZED FILTERS

Having established that the soot-loaded pressure drop of a non-catalyzed cordierite filter is minimized for high porosity and a narrow pore size distribution over the fine end of the distribution curve, the optimized pore microstructure for a catalyzed filter was investigated. In this phase of the study, six cordierite filters with a range in porosity and pore size distribution were selected and fabricated as 2-inch diameter, 6-inch long filters. The cell geometries and mercury porosimetry

data for these filters are listed in Table 1. All wall thicknesses were approximately 0.011 inches except for filter 50-8N, which was 0.019 inches. Modulus of rupture was measured by the four-point method on bars cut with their long axes parallel to the length of the channels. Filtration efficiencies for artificial soot were determined by measuring particle counts upstream and downstream of the filters using a condensation particle counter. Values are averages of readings taken over a 30-minute time span beginning three minutes after the initiation of loading.

The sample identification codes denote their approximate percent porosity, median pore diameter, and whether the pore size distribution, as defined by $(d_{50}-d_{10})/d_{50}$, is narrow (N) or broad (B) relative to an intermediate value of 0.55. Sample 60-12N was not catalyzed, but is included for comparison with the other filters.

Scanning electron micrographs of polished sections taken through the walls of filters comprised of these six materials (in some cases of different wall thickness) are shown in Figures 6a to 6f to provide visual supplementation to the data in Table 1.

Table 1
Cell geometries, physical properties, and filtration efficiencies for pre-catalyzed experimental cordierite filters

Sample Code	50-8B	50-12B	50-29B	60-12N	60-16B	60-30B
Cells/inch^2	167	182	178	183	184	189
Wall thickness (10^{-3} inches)	19.1	10.9	11.9	12.7	11.8	11.1
% Porosity	51.6	47.6	49.1	59.8	62.6	61.0
d_{10}	4.8	2.9	10.4	6.4	4.8	11.5
d_{50}	8.4	12.0	29.4	11.9	15.6	29.5
d_{90}	14.9	32.3	68.0	31.2	36.8	70.0
$(d_{50}-d_{10})/d_{50}$	0.43	0.76	0.65	0.46	0.69	0.61
Modulus of rupture (psi)	294	350	296	330	168	144
% Filtration efficiency	98.8	97.7	86.5	98.8	96.8	46.8

The six materials in Table 1 were each prepared as two filters and their clean and soot-loaded pressure drops measured by the same procedure described previously to establish a pressure drop baseline. One filter was then catalyzed using a catalyst system designated Catalyst A, and the second filter was catalyzed using a different catalyst system, Catalyst B (with the exception of Filter 60-12N). The clean and soot-loaded pressure drops of the catalyzed filters were then re-measured.

The pressure drop versus soot-loading behaviors of the bare (pre-catalyzed) and catalyzed filters measured at a flow rate of 26.25 scfm (~150,000 hr^{-1} space velocity) are presented in Figures 7a-c for filters having approximately 50% porosity, and Figures 7d-f for filters with about 60% porosity, in order of increasing median pore size.

For all filters, Catalyst A resulted in a 0 to 25% increase in soot-loaded pressure drop relative to the bare filter, whereas Catalyst B produced anywhere from a 15 to 100% increase in soot-loaded pressure drop, depending upon the filter's pore microstructure. In all cases, the increase in clean pressure drop after catalyzing is relatively small. The soot-loaded pressure drop increase after catalyzing is attributable mainly to an increase in pressure drop during the initial stages of soot loading. Thus, it may be concluded that, in those cases in which the soot-loaded pressure drop was substantially increased, the catalyst system modified the pore microstructure of the filter in such a way that the permeability of soot that deposited within the surface and near-surface pores was lowered, presumably due to a higher packing density.

Among the filters with ~50% porosity, the 50-12B filter exhibited the highest soot-loaded pressure drop in the pre-catalyzed state (Figure 7b), due to a steep increase with initial soot loading. This is consistent with this filter having the broadest pore size range in the fine end of the distribution (largest value of $(d_{50}-d_{10})/d_{50}$). Filter 50-12B also showed the greatest increase in pressure drop after catalyzing. Increasing the pore size in the 50-29B filter resulted in a lowering of the bare and catalyzed pressure drops. The unusual form of the pressure drop curves suggests a combination of "Stage 2" and "Stage 3" behavior for this coarse-porosity material, as discussed earlier in reference to Figure 1. However, the lowest bare pressure drop, and the smallest increase in pressure drop after catalyzing, were displayed by the 50-8N filter. This is consistent with the narrow pore size distribution of this filter, imparting a greater pore connectivity and possibly lower packing density of the soot in the surface and near-surface pores in this filter. The 50-8N filter further demonstrates that a narrow pore size distribution is more effective than a large pore size in providing low soot-loaded pressure drop in both a bare and catalyzed cordierite filter. Furthermore, both strength and filtration efficiency of the 50-8N filter are substantially greater than those of the coarse-porosity 50-29B filter (Table 1).

An increase in filter porosity to ~60% results in a further decrease in soot-loaded pressure drop for bare and catalyzed filters (Figures 7d-f); the reduction in clean pressure drop is relatively small. The highest pressure drop in this group is exhibited by the 60-16B filter, a higher-porosity analogue of 50-12B. Application of either catalyst system again raises the rate of pressure drop increase with initial soot loading in the surface pores (Figure 7e), but the magnitude of the effect is considerably less than for 50-12B. Increasing the median pore diameter to 30 microns in the 60-30B filter again yields a further reduction in pressure drop for both the bare and catalyzed filters. However, as observed for the 50% porosity filters, a more narrow pore size distribution in the 60-12N filter is even more effective in reducing soot-loaded pressure drop than coarsening the pore size (Figure 7d), and preserves both strength and filtration efficiency (Table 1).

The change in soot-loaded pressure drop after catalyzing for the five filters that were coated is summarized in Figure 8. For both catalyst systems, the magnitude of the increase in pressure drop after catalyzing is proportional to the pressure drop of the bare filter. Furthermore, this proportionality is non-linear, with filters having a higher pressure drop in the pre-coated state showing a greater *percent* increase in pressure drop after catalyzing. Finally, Catalyst A results in a lower pressure drop increase for all filters relative to Catalyst B, demonstrating that the catalyst system can be adjusted to minimize the pressure drop increase.

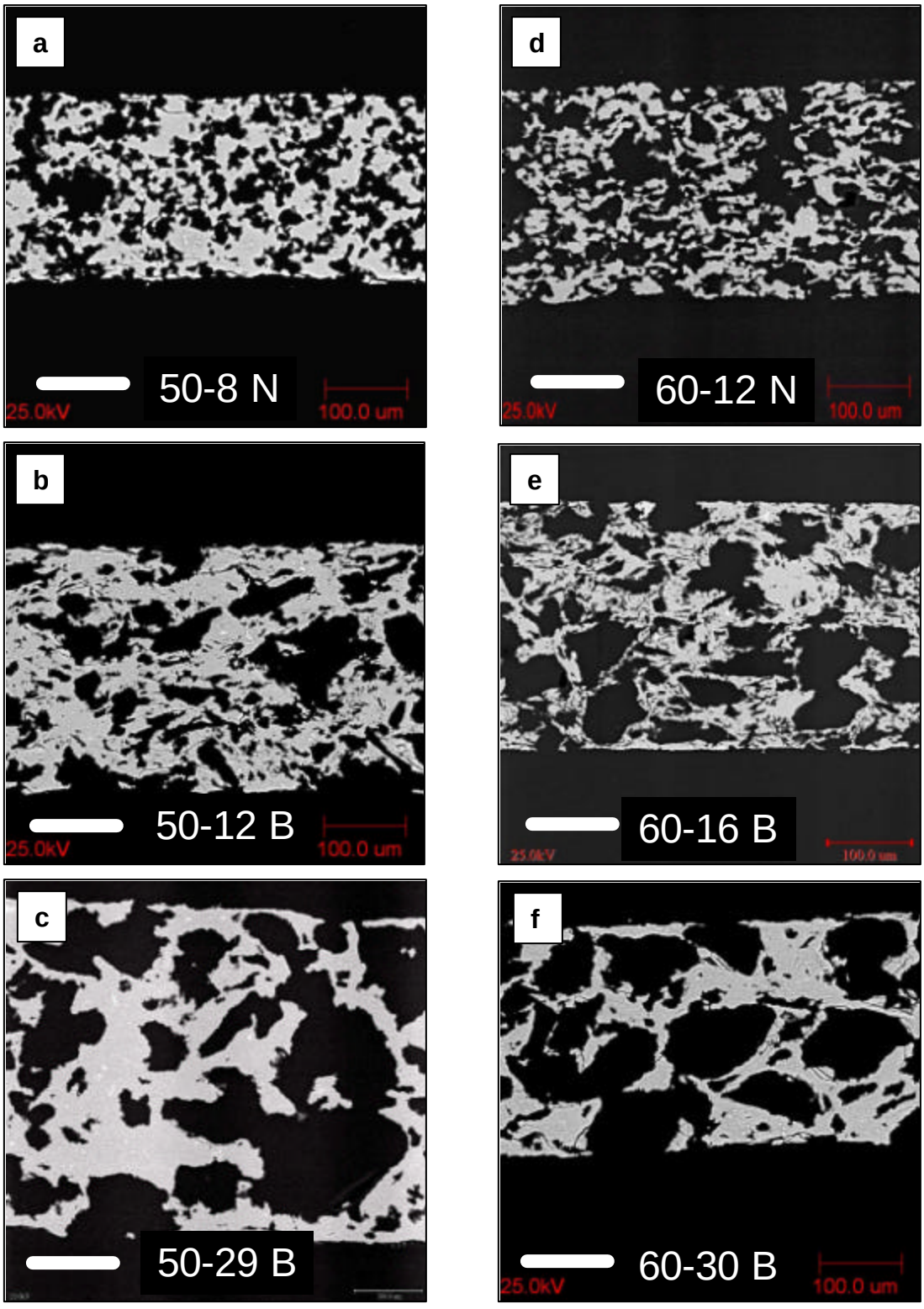

Figure 6. Back-scattered electron images of polished cross sections through non-catalyzed filter walls of six cordierite materials from Table 1. Black regions denote pores and the light gray material is predominately cordierite. Scale bar is 100 microns.

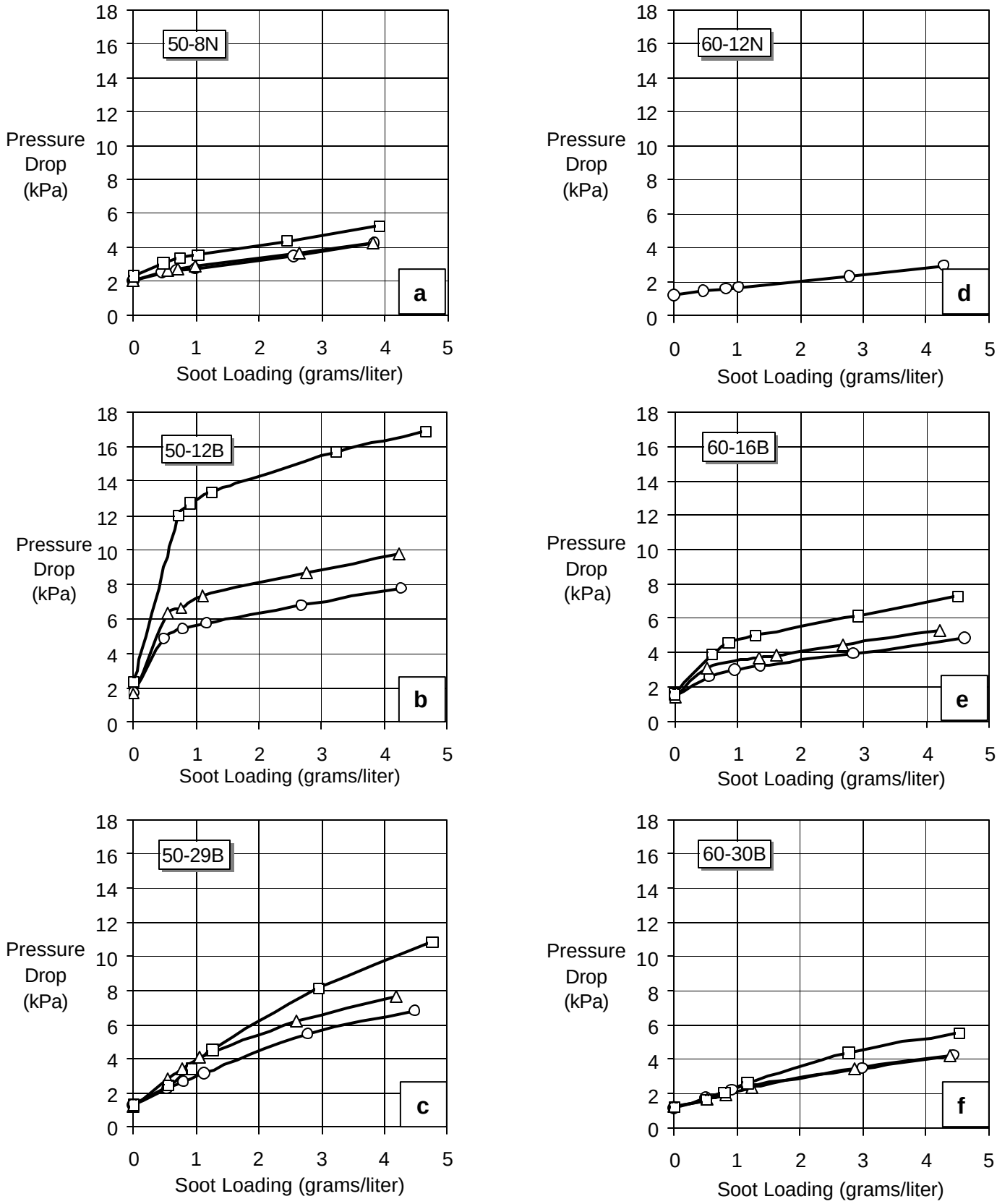

Figure 7. Pressure drop versus soot loading for pre-catalyzed cordierite filters (open circles) and filters coated with catalyst systems A (open triangles) and B (open squares) for (a) 50-8N, (b) 50-12B, (c) 50-29B, (d) 60-12N, (e) 60-16B, and (f) 60-30B filters.

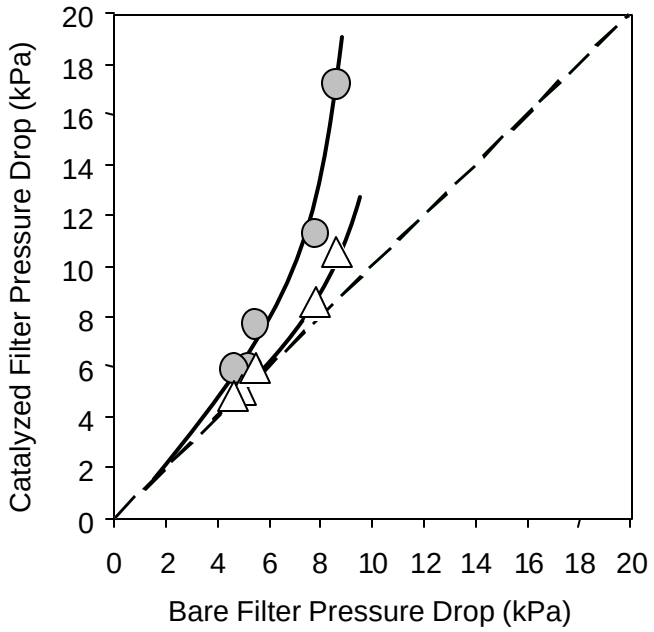

Figure 8. Pressure drops of catalyzed filters versus those of the respective bare filters at 5 g/l soot loading and a room-temperature flow rate of 26.25 scfm across a 2-inch diameter, 6-inch long filter. Open triangles denote catalyst A and filled circles indicate catalyst B.

PRESSURE DROP AND HEAT CAPACITY

As noted previously, while low pressure drop is preferred for all DPF applications, the specific engine operating conditions and regeneration strategy dictate whether the volumetric heat capacity, or "thermal mass," of the filter should be high or low.

The volumetric heat capacity of a filter is equal to the intrinsic specific heat of the crystalline material comprising the ceramic, in Joules gram^{-1} K^{-1}, multiplied by the mass of the filter, in grams, and divided by the external volume of the filter. Thus, for a cordierite filter, the mass, and hence the volumetric heat capacity, is controlled by the %porosity in the walls, the thickness of the walls, and the cell density of the filter. Other factors, such as the depth of the plugs at the ends of the alternate channels and the thickness of the outer skin on the filter also contribute to the overall filter mass. The thermal mass is not affected by the pore size distribution or pore connectivity.

Figure 9 depicts the pressure drop versus the volumetric heat capacity at 500°C for a series of cordierite filter compositions. Pressure drops pertain to 2-inch diameter, 6-inch long filters at a soot loading of 5 grams/liter and a room-temperature air flow rate of 26.25 scfm. The position of the point for the 200/12 DuraTrap^{TM} CO filter provides a starting point for comparison with the other filters. The "CO" filter is similar to the 50-12B composition in Table 1.

By improving pore connectivity while decreasing %porosity to 45% and increasing wall thickness to 0.019 inches, the pressure drop of the 200/19 DuraTrap^{TM} RC filter, discussed by Merkel et al [4], is maintained at the same value as the "CO" filter, with a 50% increase in thermal mass. The "RC" filter offers high thermal durability in applications in which uncontrolled regenerations might be anticipated.

The 200/12 DuraTrap^{TM} EC filter was developed to provide a 30% reduction in pressure drop and 15% lower thermal mass relative to the CO filter for applications in which rapid heating of a low pressure drop filter is desired.

Continued advances in understanding the relationship between pressure drop and pore microstructure of cordierite filters, coupled with optimization of the filter cell density and wall thickness, has led to the development of a new generation of filters that offer further reduction in pressure drop without sacrificing thermal mass. Two ends of the spectrum of this new family of compositions are denoted as the Developmental HTM ("High Thermal Mass") and ULPD ("Ultra-Low Pressure Drop") filters in Figure 9. Adjustments in pore microstructure and filter cell geometry enable the fabrication of a range of filters between these end points, as shown in the diagram. The combinations of pressure drop and thermal mass of these new cordierite filters overlaps those of silicon carbide filters having 42% porosity in a 200/16 cell geometry or 60% porosity in a 300/12 configuration. Based upon the relationships shown in Figure 8, it is anticipated that these cordierite filters will also exhibit low pressure drops in the catalyzed state.

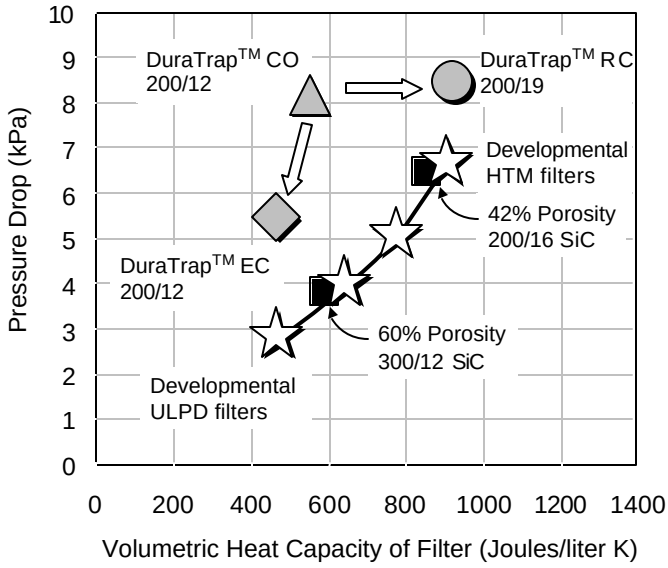

Figure 9. Pressure drops of bare filters at 5 g/l soot loading and a room-temperature flow rate of 26.25 scfm across a 2-inch diameter, 6-inch long filter, versus their volumetric heat capacities at 500°C.

SUMMARY

Experimental investigation has defined the relationship between pore microstructure and the clean and soot-loaded pressure drops of cordierite diesel particulate filters. Clean pressure drop is minimized for high porosity and, especially, large median pore size. Soot-loaded pressure drop, controlled mainly by the initial rate of pressure drop increase during the early stage of soot deposition in the surface and near-surface

pores, is minimized for high porosity and narrow pore size distribution to the fine side of the median pore diameter.

Application of catalyst systems to cordierite DPFs can, in some cases, raise the soot-loaded pressure drop. This is due mainly to an increase in the rate of pressure drop increase with initial deposition of soot in the surface and near-surface pores, implying that the catalyst system modifies the ceramic wall pore microstructure in such a way as to result in denser packing of the soot in the surface pores. Generally, the soot-loaded pressure drop of the catalyzed filter is proportional to that of the pre-coated filter. However, the proportionality is non-linear, with a higher percent increase for catalyzed filters that have a high bare pressure drop. By appropriate modification of the catalyst system, acceptable pressure drops could be obtained for all filters investigated.

For either a bare or catalyzed filter, the soot-loaded pressure drop is reduced by increased porosity and either a coarse pore size or a narrow pore size distribution. A narrow pore size distribution, centered on a median pore diameter of less than 20 μm, is preferable to coarser pore filters because high filtration efficiency and greater fracture strength are maintained. Thus, for sufficiently narrow pore size, very coarse pores and high porosities are not required to maintain low soot-loaded pressure drop in either the bare or catalyzed state.

REFERENCES

1. Murtagh, M.J., Sherwood, D.L., and Socha, L.S., Jr., 1994, "Development of a Diesel Particulate Filter Composition and Its Effect on Thermal Durability and Filtration Performance," SAE Technical Paper 940235.
2. Masoudi, M., Konstandopoulos, A.G., Nikitidis, M.S., Skaperdas, E., Zarvalis, D., Kladopoulou, E., and Altiparmakis, C., 2001, "Validation of a Model and Development of a Simulator for Predicting the Pressure Drop of Diesel Particulate Filters," SAE Technical Paper 2001-01-0911.
3. Scheidegger, A.E. , 1960, *The Physics of Flow through Porous Media*, The MacMillan Company, New York
4. Merkel, G.A., Beall, D.M., Hickman, D.L., and Vemacotola, M.J., 2001, "Effects of Microstructure and Cell Geometry on Performance of Cordierite Diesel Particulate Filters," SAE Technical Paper 2001-01-0193.